Relativistic corrections to paired production of charmonium and bottomonium in decays of the Higgs boson

R. N. Faustov,[1] A. P. Martynenko,[2] and F. A. Martynenko[2]

[1]*Institute of Cybernetics and Informatics in Education, FRC CSC RAS, Moscow 119333, Russia*
[2]*Samara University, Samara 443086, Russia*

(Received 3 October 2022; accepted 10 February 2023; published 1 March 2023)

The rare decay process of the Higgs boson into a pair of J/Ψ and Υ particles is studied within the perturbative Standard Model and the relativistic quark model. The relativistic corrections connected with the relative motion of quarks are calculated in the production amplitude and the wave functions of the bound states. Numerical values of the decay widths of the Higgs boson are obtained, which can be used for comparison with experimental data.

DOI: 10.1103/PhysRevD.107.056002

I. INTRODUCTION

Since the discovery of the Higgs boson [1,2], a period of detailed study of the various processes connected with this particle has begun. We can say that the study of the Higgs sector has become one of the most important areas in particle physics [3]. The discovery of the Higgs boson confirmed the electroweak mechanism of symmetry breaking, but the nature of this particle remains to be explored. To do this, it is necessary to create particle colliders, on which Higgs bosons could be produced in significant quantities, which would make it possible to proceed to a precise study of the parameters of the Higgs sector. It is possible that interaction processes involving the Higgs boson can provide a transition to a new physics that lies beyond the Standard Model.

Among the parameters of the Higgs sector, the coupling constants of the Higgs boson with various bosons [$g(HZZ)$, $g(HWW)$], leptons [$g(H\tau\tau)$, $g(H\mu\mu)$], and quarks [$g(Hcc)$, $g(Hbb)$], stand out. They determine the decay processes of the Higgs boson into various particles [4]. Due to the Higgs boson large mass and the presence of coupling constants with different particles, the Higgs boson has numerous decay channels. The decay channel of the Higgs boson into a pair of heavy quarks is interesting because it creates the possibility of the production of bound states of heavy quarks. Thus, rare exclusive decay processes of the Higgs boson into a pair of charmonium or bottomonium are of obvious interest both for studying the decay mechanisms and for studying the properties of bound states of quarks. Here it is useful to recall that the study of charmonium pair production in electron-positron annihilation played an important role in its time in explaining the mechanism of such a reaction, as well as in understanding the role of various effects in calculating the observed paired production cross sections [5,6].

The CMS Collaboration began the search for rare Higgs decays into a pair of heavy vector quarkonia in 2019 [7]. The results of new upper limits on the branching fractions were obtained in [8],

$$B(H \to J/\Psi, J/\Psi) < 3.8 \times 10^{-4}, \tag{1}$$

$$B(H \to \Upsilon(1S), \Upsilon(1S)) < 1.7 \times 10^{-3}. \tag{2}$$

Theoretical studies of the production of a pair of heavy quarkonia in the decays of the Higgs boson began about 40 years ago in [9,10]. In these papers, theoretical formulas were obtained for estimating the decay widths in the nonrelativistic approximation for some decay mechanisms; more recent theoretical studies of these processes were carried out in [11–14].

In this work we continue the study of relativistic effects in the exclusive paired charmonium and bottomonium production in the Higgs boson decay which began in [12,13] for B_c mesons. Our calculation of the decay widths is performed on the basis of relativistic-quark model used previously for the investigation of relativistic corrections in different reactions in [15–17], including pair production of mesons and baryons in electron-positron annihilation and proton-proton interaction. Despite the rare nature of the Higgs boson decays being studied, one can hope that such processes can be investigated at the new Higgs boson factories. The purpose of this paper is to perform a new analysis of the vector quarkonium pair production processes in Higgs boson decays in the Standard Model and to

obtain numerical estimates of the corresponding decay widths.

In comparison with previous works [11,14] we have performed a more detailed consideration of various mechanisms (quark-gluon, quark-photon, photon-photon and Z-bosonic mechanisms) of charmonium and bottonium pair production. Additionally, in our calculation, we take into account the relativistic corrections connected with the relative motion of heavy quarks, both in the quark-antiquark production amplitude itself and in the wave functions of bound states.

As a result, new numerical estimations for the Higgs boson decay rates are obtained. An experimental study of these rare exclusive decays of the Higgs boson at future high-luminosity colliders could be useful in testing the Standard Model with higher accuracy.

II. GENERAL FORMALISM

From the very beginning, it should be emphasized that there are several groups of amplitudes for the decay of the Higgs boson with the formation of a pair of charmoniums J/Ψ (bottomonium Υ), which contribute the same order of magnitude to the decay width. We study the amplitudes which are shown in Figs. 1–5. They represent different decay mechanisms with pair vector meson production; quark-gluon, quark-photon, quark-loop, W-boson loop, and Z-boson. The first group includes quark-gluon amplitudes shown in Fig. 1 (quark-gluon mechanism). The factor determining the order of contributions can be represented as α_s/M_H^4, where M_H is the mass of the Higgs boson. Such a factor can be distinguished from the very beginning due to the structure of the interaction vertices and the denominators of the particle propagators. The second group is formed by quark-photon amplitudes shown in Fig. 2 (quark-photon mechanism). The order of contribution is determined here by the factor $\alpha/M_H^2 M_{\mathcal{Q}\bar{\mathcal{Q}}}^2$. The third group is formed by the amplitudes in Figs. 3 and 4 which contain the quark or W-boson loop with two photons that create a pair of J/Ψ (or Υ) mesons (quark-loop and W-boson loop mechanisms). The primary common factor in this case takes the form $\alpha^2/M_{\mathcal{Q}\bar{\mathcal{Q}}}^4$. Finally, the last group of amplitudes in Fig. 5 is determined by the interaction of the Higgs boson with a pair of Z-bosons (Z-boson mechanism). To achieve good calculation accuracy, it is necessary to take into account the contribution of all amplitudes from these groups.

Let us consider firstly the Higgs boson decay amplitudes shown in Figs. 1 and 2. For pair production of quarkonia in the leading order of perturbation theory, it is necessary to obtain two free quarks and two free antiquarks at the first stage. Then they can form bound states with some probability at the next stage. In the quasipotential approach the decay amplitude can be presented as a convolution of a perturbative production amplitude of two c-quark and $\bar{c}$-antiquark pairs and the quasipotential wave functions of the final mesons [12,13],

$$\begin{aligned}\mathcal{M}(P,Q) = -i(\sqrt{2}G_F)^{\frac{1}{2}}\frac{2\pi}{3}M_{\mathcal{Q}\bar{\mathcal{Q}}}\int\frac{d\mathbf{p}}{(2\pi)^3}\int\frac{d\mathbf{q}}{(2\pi)^3}\\ \times \mathrm{Tr}\{\Psi^{\mathcal{V}}(p,P)\Gamma_1^{\nu}(p,q,P,Q)\Psi^{\mathcal{V}}(q,Q)\gamma_{\nu}\\ + \Psi^{\mathcal{V}}(q,Q)\Gamma_2^{\nu}(p,q,P,Q)\Psi^{\mathcal{V}}(p,P)\gamma_{\nu}\},\end{aligned} \tag{3}$$

where $M_{\mathcal{Q}\bar{\mathcal{Q}}}$ is the mass of quarkonium. Four-momenta p_1 and p_2 of c-quark and $\bar{c}$-antiquark in the pair forming the first $(\mathcal{Q}\bar{\mathcal{Q}})$ meson, and four-momenta q_2 and q_1 for quark and antiquark in the second meson $(\mathcal{Q}\bar{\mathcal{Q}})$ are expressed in terms of relative and total four momenta as follows:

$$\begin{aligned}p_{1,2} &= \frac{1}{2}P \pm p, \qquad (pP) = 0;\\ q_{1,2} &= \frac{1}{2}Q \pm q, \qquad (qQ) = 0.\end{aligned} \tag{4}$$

A superscript $\mathcal{V}$ indicates a vector meson $(\mathcal{Q}\bar{\mathcal{Q}})$. The vertex functions $\Gamma_{1,2}$ are presented below in leading order and in Fig. 1. Heavy quarks c, b, and antiquarks $\bar{c}$, $\bar{b}$, are outside the mass shell in the intermediate state; $p_{1,2}^2 \neq m^2$, so that $p_1^2 - m^2 = p_2^2 - m^2$, which means that there is a symmetrical exit of particles from the mass shell.

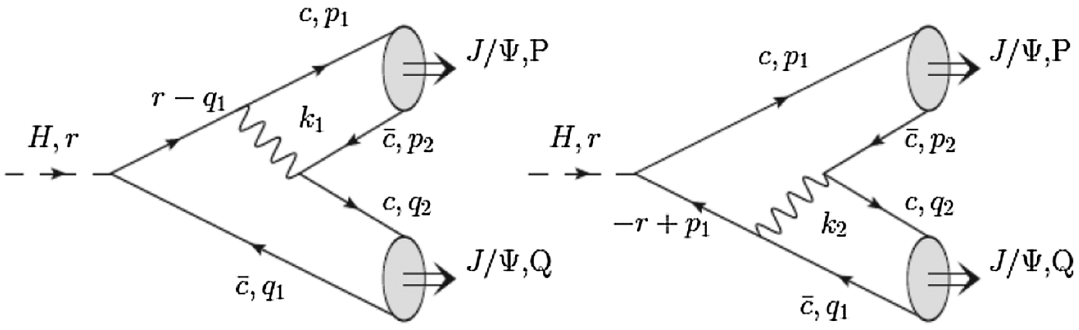

FIG. 1. Quark-gluon mechanism of the pair charmonium production in the Higgs boson decay. Dashed line shows the Higgs boson and wavy line corresponds to the gluon.

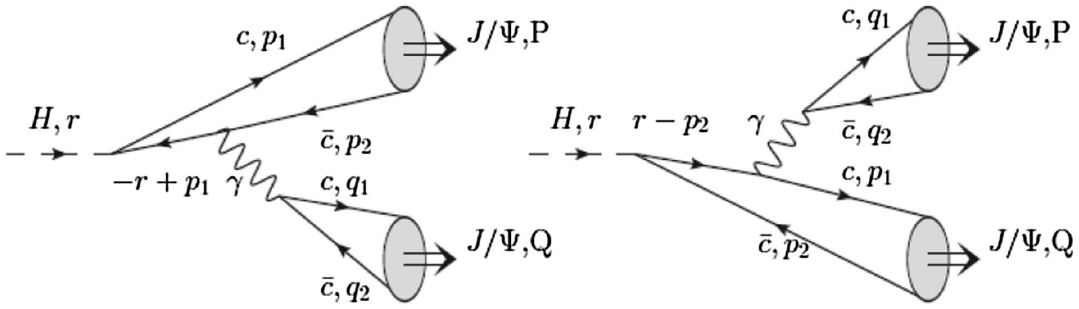

FIG. 2. Quark-photon mechanism of the pair charmonium production in the Higgs boson decay. Dashed line shows the Higgs boson and wavy line corresponds to the photon.

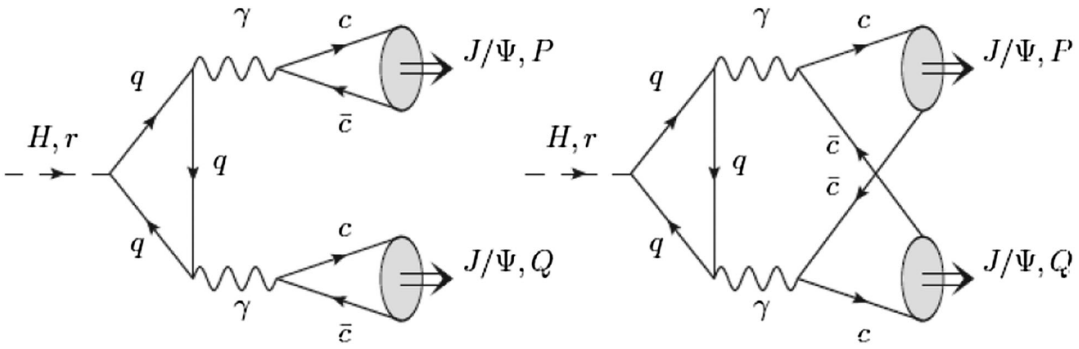

FIG. 3. Quark loop mechanism of the pair charmonium production in the Higgs boson decay. Dashed line shows the Higgs boson and wavy line corresponds to the photon.

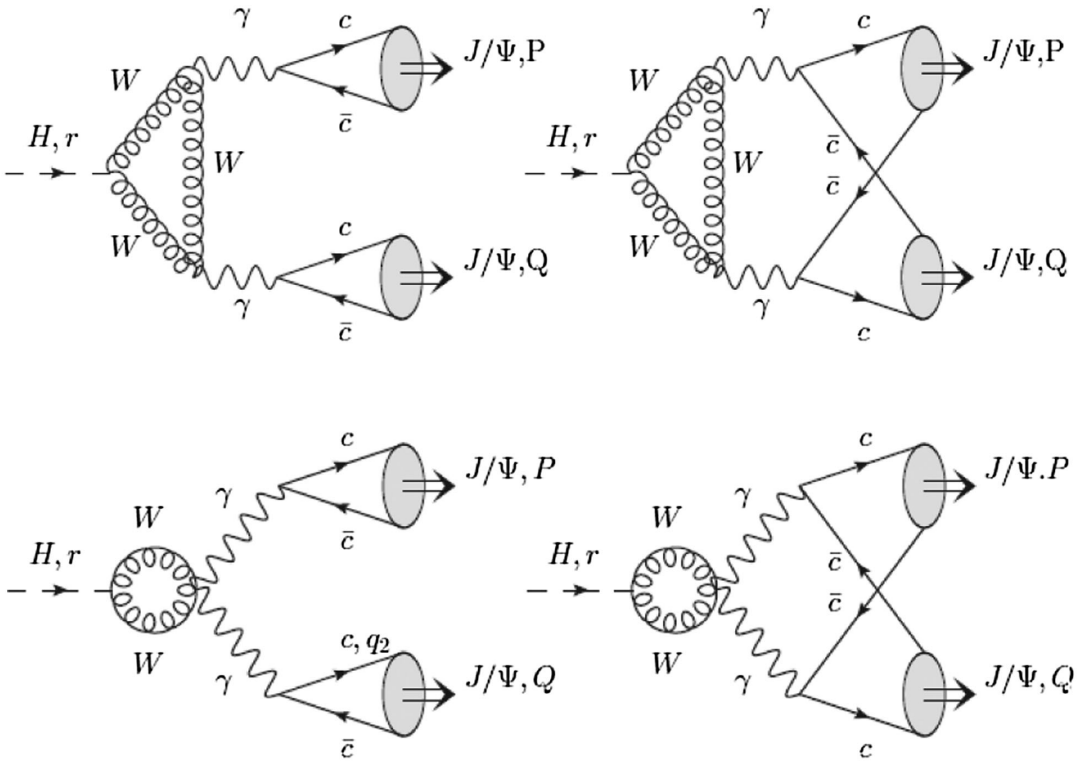

FIG. 4. W-boson loop mechanism of the pair charmonium production in the Higgs boson decay. Dashed line shows the Higgs boson and wavy line corresponds to the photon.

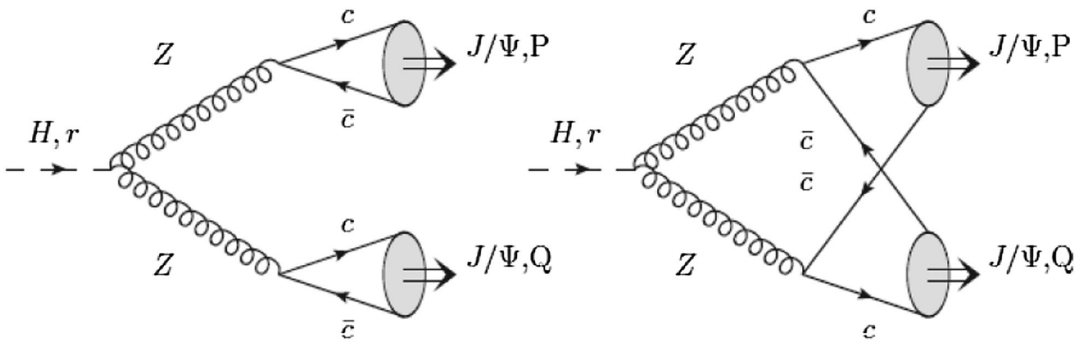

FIG. 5. Z-boson mechanism of the pair charmonium production in the Higgs boson decay. Dashed line shows the Higgs boson and wavy line corresponds to the Z-boson.

In Eq. (3) we integrate over the relative three-momenta of quarks and antiquarks in the final state. The systematic account of all terms depending on the relative quark momenta p and q in the decay amplitude is important for increasing the accuracy of the calculation. $p = L_P(0, \mathbf{p})$ and $q = L_Q(0, \mathbf{q})$ are the relative four-momenta obtained by the Lorentz transformation of four-vectors $(0, \mathbf{p})$ and $(0, \mathbf{q})$ to the reference frames moving with the four-momenta P and Q.

The relativistic wave functions of the bound quarks accounting for the transformation from the rest frame to the moving one with four momenta P, and Q, are

$$\Psi(p,P) = \frac{\Psi_0(\mathbf{p})}{\left[\frac{\epsilon(p)}{m}\frac{\epsilon(p)+m}{2m}\right]}\left[\frac{\hat{v}_1-1}{2} + \hat{v}_1\frac{\mathbf{p}^2}{2m(\epsilon(p)+m)} - \frac{\hat{p}}{2m}\right] \times \hat{\varepsilon}(P,S_z) \quad (1+\hat{v}_1)\left[\frac{\hat{v}_1+1}{2} + \hat{v}_1\frac{\mathbf{p}^2}{2m(\epsilon(p)+m)} + \frac{\hat{p}}{2m}\right], \quad (5)$$

$$\Psi(q,Q) = \frac{\Psi_0(\mathbf{q})}{\left[\frac{\epsilon(q)}{m}\frac{\epsilon(q)+m}{2m}\right]}\left[\frac{\hat{v}_2-1}{2} + \hat{v}_2\frac{\mathbf{q}^2}{2m(\epsilon(q)+m)} + \frac{\hat{q}}{2m}\right] \times \hat{\varepsilon}(Q,S_z) \quad (1+\hat{v}_2)\left[\frac{\hat{v}_2+1}{2} + \hat{v}_2\frac{\mathbf{q}^2}{2m(\epsilon(q)+m)} - \frac{\hat{q}}{2m}\right], \quad (6)$$

where the hat symbol means a contraction of the four-vector with the Dirac gamma matrices; $v_1 = P/M_{Q\bar{Q}}$, $v_2 = Q/M_{Q\bar{Q}}$; $\epsilon(p) = \sqrt{m^2+\mathbf{p}^2}$, m is $c(b)$-quark mass, and $M_{Q\bar{Q}}$ is the mass of charmonium (bottomonium) state. $\varepsilon^\lambda(P,S_z)$ is the polarization vector of the $J/\Psi(\Upsilon)$ meson.

Expressions (5) and (6) represent complicated functions depending on relative momenta $\mathbf{p}$, $\mathbf{q}$ including the bound state wave function in the rest frame $\Psi_0(\mathbf{p})$. The color part of the meson wave function in the amplitudes (5)–(6) is taken as $\delta_{ij}/\sqrt{3}$ (color indexes i, j, $k = 1, 2, 3$).

The general structure of expressions (5)–(6) allows us to say that they are the product of the wave functions of mesons in the rest frame and special projection operators resulting from the transformation from the moving reference frame to the reference frame in which the meson is at rest. Expressions (5)–(6) make it possible to correctly take into account the relativistic corrections connected with the relative momenta of quarks in the final states. It is useful to note that the expression for the projection operators was obtained in the framework of nonrelativistic quantum chromodynamics in [18] in a slightly different form for the case when the quark momenta lie on the mass shell. The transformation law of the bound state wave functions of quarks, which is used in the derivation of equations (5)–(6), was obtained in the Bethe-Salpeter approach in [19] and in quasipotential method in [20].

As follows from (5)–(6), when constructing the decay amplitudes of the Higgs boson, projection operators are introduced for quark-antiquark pairs onto the spin states with total spin $S = 1$ of the following form:

$$\hat{\Pi}^{\mathcal{V}} = [v_2(0)\bar{u}_1(0)]_{S=1} = \hat{\varepsilon}\frac{1+\gamma^0}{2\sqrt{2}}. \quad (7)$$

Total amplitude of the Higgs boson decay to paired vector quarkonium in the case of quark-gluon mechanism in the leading order in strong coupling constant α_s can be presented in the form,

$$\mathcal{M} = \frac{4\pi}{3}M_{Q\bar{Q}}\alpha_s\Gamma_Q\int\frac{d\mathbf{p}}{(2\pi)^3}\int\frac{d\mathbf{q}}{(2\pi)^3}\mathrm{Tr}\{\mathcal{T}_{12}+\mathcal{T}_{34}\}, \quad (8)$$

$$\mathcal{T}_{12} = \Psi^{\mathcal{V}}(p,P)\left[\frac{\hat{p}_1-\hat{r}+m}{(r-p_1)^2-m^2}\gamma_\mu + \gamma_\mu\frac{\hat{r}-\hat{q}_1+m}{(r-q_1)^2-m^2}\right] \times D^{\mu\nu}(k_2)\Psi^{\mathcal{V}}(q,Q)\gamma_\nu, \quad (9)$$

$$\mathcal{T}_{34} = \Psi^{\mathcal{V}}(q,Q)\left[\frac{\hat{p}_2-\hat{r}+m}{(r-p_2)^2-m^2}\gamma_\mu + \gamma_\mu\frac{\hat{r}-\hat{q}_2+m}{(r-q_2)^2-m^2}\right] \times D^{\mu\nu}(k_1)\Psi^{\mathcal{V}}(p,P)\gamma_\nu, \quad (10)$$

where $\alpha_s = \alpha_s(\frac{M_H^2}{4\Lambda^2})$, $\Gamma_Q = m(\sqrt{2}G_F)^{\frac{1}{2}}$.

The four-momentum of the Higgs boson squared is $r^2 = M_H^2 = (P+Q)^2 = 2M_{Q\bar{Q}}^2 + 2PQ$. The gluon four-momenta are $k_1 = p_1 + q_1$, $k_2 = p_2 + q_2$. Relative momenta p, q of heavy quarks enter in the gluon propagators $D_{\mu\nu}(k_{1,2})$ and quark propagators as well as in relativistic wave functions (5) and (6). Accounting for the small ratio of relative quark momenta p and q to the mass of the Higgs boson M_H, we can simplify the denominators of quark and gluon propagators as follows:

$$\frac{1}{(p_1+q_1)^2} \approx \frac{1}{(p_2+q_2)^2} = \frac{4}{M_H^2}, \tag{11}$$

$$\frac{1}{(r-q_1)^2 - m_1^2} = \frac{1}{(-r-p_1)^2 - m_1^2} = \frac{1}{(r-p_2)^2 - m_1^2} = \frac{1}{(-r-q_2)^2 - m_1^2} = \frac{2}{M_H^2}. \tag{12}$$

In (11)–(12) we completely neglect corrections of the form $|\mathbf{p}|/M_H$, $|\mathbf{q}|/M_H$. At the same time, we keep in the amplitudes (9) and (10) the second-order correction for small ratios $|\mathbf{p}|/m$, $|\mathbf{q}|/m$ relative to the leading-order result. Calculating the trace in obtained expression in the package FORM [21], we find relativistic amplitudes of the paired meson production in the form:

$$\mathcal{M}_{\mathcal{V}\mathcal{V}}{}^{(1)} = \frac{256\pi}{3M_H^4}(\sqrt{2}G_F)^{\frac{1}{2}} m M_{Q\bar{Q}} \alpha_s \varepsilon_1^\lambda \varepsilon_2^\sigma F_{1,\mathcal{V}\mathcal{V}}^{\lambda\sigma} |\tilde{\Psi}_\mathcal{V}(0)|^2, \tag{13}$$

where ε_1^λ, ε_2^σ are the polarization vectors of spin-1 mesons. The superscript in amplitude designation and subscript in tensor function $F_{1,\mathcal{V}\mathcal{V}}^{\lambda\sigma}$ designation denotes the contribution of the quark-gluon mechanism in Fig. 1. An explicit expression for the function $F_{1,\mathcal{V}\mathcal{V}}^{\lambda\sigma}$ is presented in Eq. (19).

The contribution of the amplitudes in Fig. 2 $\mathcal{M}_{\mathcal{V}\mathcal{V}}{}^{(2)}$ to the total decay amplitude must also be taken into account, because these amplitudes have the same order as the previous ones, despite the replacement $\alpha_s \to \alpha$. This is due to the presence in the denominator of the mass of the meson instead of the mass of the Higgs boson [22]. The expression for the production amplitudes of the pair J/Ψ (Υ) has a similar structure with slight changes in the common factors,

$$\mathcal{M}_{\mathcal{V}\mathcal{V}}{}^{(2)} = \frac{288\pi}{M_H^2 M_{Q\bar{Q}}}(\sqrt{2}G_F)^{\frac{1}{2}} m e_Q^2 \alpha \varepsilon_1^\lambda \varepsilon_2^\sigma F_{2,\mathcal{V}\mathcal{V}}^{\lambda\sigma} |\tilde{\Psi}_\mathcal{V}(0)|^2, \tag{14}$$

where the function $F_{2,\mathcal{V}\mathcal{V}}^{\lambda\sigma}$ has the same general form as the function $F_{1,\mathcal{V}\mathcal{V}}^{\lambda\sigma}$ [see (19)].

The tensor corresponding to the quark or W-boson loops in Figs. 3 and 4 has the structure (the subscript denotes the contribution of the quark or bosonic loop),

$$T_{Q,W}^{\mu\nu} = A_{Q,W}(t)(g^{\mu\nu}(v_1 v_2) - v_1^\nu v_2^\mu) + B_{Q,W}(t)[v_2^\mu - v_1^\mu(v_1 v_2)][v_1^\nu - v_2^\nu(v_1 v_2)], \tag{15}$$

where $t = \frac{M_h^2}{4m_Q^2}$ or $t = \frac{M_h^2}{4m_W^2}$, m_W is the mass of W boson, m_Q is the mass of heavy quark in the quark loop. The structure functions $A_{Q,W}(t)$, $B_{Q,W}(t)$ can be obtained using an explicit expression for a loop integrals (see Appendixes A and B).

The amplitudes in Figs. 3–5 with quark, W-boson loops, and ZZ in an intermediate state contain the contributions of direct (left) and crossed (right) diagrams. The direct diagrams, in which virtual photons or Z-bosons give vector quarkonia in the final state, are dominant in terms of the mass factor. However, the structure of the numerators of the direct and cross amplitudes is different, which can eventually lead to numerically close contributions. In what follows, we present the expressions for these amplitudes only in the leading order:

$$\mathcal{M}_{\mathcal{V}\mathcal{V}}{}^{(3)} = \frac{2052\pi^2}{m_Q M_{Q\bar{Q}}}(\sqrt{2}G_F)^{\frac{1}{2}} e_q^2 e_Q^2 \alpha^2 \varepsilon_1^\lambda \varepsilon_2^\sigma F_{3,\mathcal{V}\mathcal{V}}^{\lambda\sigma} |\tilde{\Psi}_\mathcal{V}(0)|^2, \tag{16}$$

$$\mathcal{M}_{\mathcal{V}\mathcal{V}}{}^{(4)} = \frac{48\pi^2 M_Z M_W}{M_{Q\bar{Q}}^4}(\sqrt{2}G_F)^{\frac{1}{2}} e_q^2 \alpha^2 \times \cos\theta_W \varepsilon_1^\lambda \varepsilon_2^\sigma F_{4,\mathcal{V}\mathcal{V}}^{\lambda\sigma} |\tilde{\Psi}_\mathcal{V}(0)|^2, \tag{17}$$

$$\mathcal{M}_{\mathcal{V}\mathcal{V}}{}^{(5)} = \frac{48\pi\alpha}{M_Z^2 \sin^2 2\theta_W}(\sqrt{2}G_F)^{\frac{1}{2}} \varepsilon_1^\lambda \varepsilon_2^\sigma F_{5,\mathcal{V}\mathcal{V}}^{\lambda\sigma} |\tilde{\Psi}_\mathcal{V}(0)|^2, \tag{18}$$

where m is the mass of heavy quark c, b, produced in the vertex of Higgs boson decay, e_q is the charge (in units e) of heavy quark (c or b) entering in final mesons, e_Q is the charge (in units e) of heavy quark (c, b or t) in the quark loop.

The tensor functions in amplitudes (13)–(18) have the following form:

$$F_{i,\mathcal{V}\mathcal{V}}^{\alpha\beta} = g_1^{(i)} v_1^\alpha v_2^\beta + g_2^{(i)} g^{\alpha\beta}, \qquad g_1^{(1)} = -2 + \frac{2}{9}\omega_1^2, \tag{19}$$

$$g_2^{(1)} = -1 - 2r_2 + r_1^2 + \frac{4}{3}r_2\omega_1 + \frac{1}{9}\omega_1^2 + \frac{2}{3}r_2\omega_1^2 - \frac{1}{9}r_1^2\omega_1^2,$$
$$g_1^{(2)} = 4 - \frac{4}{9}\omega_1^2, \qquad g_2^{(2)} = 2 + 4r_2 - 2r_1^2 - \frac{8}{3}r_2\omega_1 - \frac{2}{9}\omega_1^2 - \frac{4}{3}r\omega_1^2 + \frac{2}{9}r_1^2\omega_1^2, \tag{20}$$

$$g^{(3)}_{1,Q} = -A_Q(t)\left(1+\frac{2}{3}\omega_1+\frac{1}{9}\omega_1^2\right)+B_Q(t)\left(1+\frac{2}{3}\omega_1+\frac{1}{9}\omega_1^2\right), \tag{21}$$

$$g^{(3)}_{2,Q} = A_Q(t)\left(-1-\frac{2}{3}\omega_1-\frac{1}{9}\omega_1^2+\frac{1}{2}r_1^2+\frac{1}{3}\omega_1 r_1^2+\frac{1}{18}\omega_1^2 r_1^2\right),$$

$$g^{(4)}_{1} = -A_W(t)\left(1+\frac{2}{3}\omega_1+\frac{1}{9}\omega_1^2\right)+B_W(t)\left(1+\frac{2}{3}\omega_1+\frac{1}{9}\omega_1^2\right), \tag{22}$$

$$g^{(4)}_{2} = A_W(t)\left(-1-\frac{2}{3}\omega_1-\frac{1}{9}\omega_1^2+\frac{1}{2}r_1^2+\frac{1}{3}\omega_1 r_1^2+\frac{1}{18}\omega_1^2 r_1^2\right), \tag{23}$$

$$g^{(5)}_{2} = \left(1+\frac{1}{3}\omega_1\right)^2\left(\frac{1}{2}-a_z\right)^2-\frac{M_z^4}{3\left(\frac{M_h^2}{4}-M_Z^2\right)^2}\left(-\frac{1}{4}-\frac{1}{6}\omega_1-\frac{1}{36}\omega_1^2\right.$$
$$\left.+\frac{1}{2}a_z+\frac{1}{3}\omega_1 a_z+\frac{1}{18}\omega_1^2 a_z-\frac{1}{2}a_z^2-\frac{1}{3}\omega_1 a_z^2-\frac{1}{18}\omega_1^2 a_z^2\right), \qquad g^{(5)}_1 = 0, \tag{24}$$

where the parameter $r_1 = \frac{M_H}{M_{Q\bar{Q}}}$, $r_2 = \frac{m}{M_{Q\bar{Q}}}$, $a_z = 2|e_Q|\sin^2\theta_W$. The superscript of the functions $g^{(i)}_{1,2}$ corresponds to a certain decay mechanism, shown in Figs. 1–5. Expressions (19)–(24) contain, after all transformations of the Higgs boson decay amplitudes, a set of relativistic parameters ω_n that determine the magnitude of relativistic effects in these amplitudes. Within the framework of the relativistic quark model, we can find their numerical values. The precise determination of the parameters ω_n and their calculation are discussed in more detail in Sec. III.

The decay widths of the Higgs boson into a pair of vector quarkonia states are determined by the following expressions (see also [12,13]):

$$\Gamma_{\mathcal{V}\mathcal{V}} = \frac{2^{14}\sqrt{2}\pi\alpha_s^2 m^2 G_F|\tilde{\Psi}_{\mathcal{V}}(0)|^4\sqrt{\frac{r_1^2}{4}-1}}{9M_H^5 r_1^5}\sum_{\lambda,\sigma}|\varepsilon_1^\lambda\varepsilon_2^\sigma F^{\lambda\sigma}_{\mathcal{V}\mathcal{V}}|^2, \tag{25}$$

$$F^{\lambda\sigma}_{\mathcal{V}\mathcal{V}} = \left[g_1^{(1)}+\frac{9}{16}r_1^2\frac{e_q^2\alpha}{\alpha_s}g_1^{(2)}+\sum_Q\frac{27\pi}{8}r_1^4\frac{e_Q^2e_q^2\alpha^2m_Q^2}{\alpha_s m M_{Q\bar{Q}}}g^{(3)}_{1,Q}+\frac{9\pi e_q^2\alpha^2 r_1^4 M_Z M_W}{64\alpha_s m M_{Q\bar{Q}}}g_1^{(4)}\right.$$
$$\left.+\frac{9M_H^4\alpha}{16M_Z^2 m M_{Q\bar{Q}}\alpha_s}\frac{(\frac{1}{2}-2|e_q|\sin^2\theta_W)^2}{\sin^2 2\theta_W}g_1^{(5)}\right]v_1^\sigma v_2^\lambda+\left[g_2^{(1)}+\frac{9}{16}r_1^2\frac{e_q^2\alpha}{\alpha_s}g_2^{(2)}+\sum_Q\frac{27\pi}{8}r_1^4\frac{e_q^2e_Q^2\alpha^2m_Q^2}{\alpha_s m M_{Q\bar{Q}}}g^{(3)}_{2,Q}\right.$$
$$\left.+\frac{9\pi e_q^2\alpha^2 r_1^4 M_Z M_W}{64\alpha_s m M_{Q\bar{Q}}}\cos\theta_W g_2^{(4)}+\frac{9M_H^4\alpha}{16M_Z^2 m M_{Q\bar{Q}}\alpha_s}\frac{1}{\sin^2 2\theta_W}g_2^{(5)}\right]g^{\lambda\sigma}. \tag{26}$$

We found it convenient to separate in square brackets in (26) the coefficients denoting the relative contribution of different decay mechanisms with respect to the quark-gluon mechanism in Fig. 1. The common factor in (25) corresponds to the amplitudes of the quark-gluon decay mechanism.

III. NUMERICAL RESULTS

General expression for the decay rate (25) contains numerous parameters. One part of the parameters, such as quark masses or the masses of mesons, are determined within the framework of quark models as a result of calculating the observed quantities. The parameters of quark models are found from the condition of the best agreement with experimental data [4]. Another part of the relativistic parameters ω_n can also be found in the quark model as a result of calculating integrals with wave functions of quark bound states in the momentum representation. Thus, we can say that the approach to calculation based on the relativistic quark model is closed, because it allows to calculate all the necessary parameters without resorting to additional hypotheses.

To calculate ω_n, we assume that the dynamics of quark-antiquark pairs is determined by the QCD generalization of the standard Breit-Hamiltonian in the center-of-mass reference frame [23–29],

$$H = H_0 + \Delta U_1 + \Delta U_2, \qquad H_0 = 2\sqrt{\mathbf{p}^2 + m^2} - 2m - \frac{C_F\tilde{\alpha}_s}{r} + Ar + B, \tag{27}$$

$$\Delta U_1(r) = -\frac{C_F\alpha_s^2}{4\pi r}[2\beta_0 \ln(\mu r) + a_1 + 2\gamma_E\beta_0], \qquad a_1 = \frac{31}{3} - \frac{10}{9}n_f, \qquad \beta_0 = 11 - \frac{2}{3}n_f, \tag{28}$$

$$\Delta U_2(r) = -\frac{C_F\alpha_s}{2m^2 r}\left[\mathbf{p}^2 + \frac{\mathbf{r}(\mathbf{rp})\mathbf{p}}{r^2}\right] + \frac{\pi C_F\alpha_s}{m^2}\delta(\mathbf{r}) + \frac{3C_F\alpha_s}{2m^2 r^3}(\mathbf{SL}) - \frac{C_F\alpha_s}{2m^2}\left[\frac{\mathbf{S}^2}{r^3} - 3\frac{(\mathbf{Sr})^2}{r^5} - \frac{4\pi}{3}(2\mathbf{S}^2 - 3)\delta(\mathbf{r})\right] - \frac{C_A C_F\alpha_s^2}{2mr^2}, \tag{29}$$

where $\mathbf{L} = [\mathbf{r} \times \mathbf{p}]$, $\mathbf{S} = \mathbf{S}_1 + \mathbf{S}_2$, n_f is the number of flavors, $C_A = 3$ and $C_F = 4/3$ are the color factors of the SU(3) color group, $\gamma_E \approx 0.577216$ is the Euler constant. To describe the hyperfine structure of the energy spectrum, the following confinement potential is usually added to (27) [30–32]:

$$\Delta V^{hfs}_{\text{conf}}(r) = f_V\left[\frac{A}{2m^2 r}\left(1 + \frac{8}{3}\mathbf{S}_1\mathbf{S}_2\right) + \frac{3A}{2m^2 r}\mathbf{LS} + \frac{A}{3m^2 r}\left(\frac{3}{r^2}(\mathbf{S}_1\mathbf{r})(\mathbf{S}_2\mathbf{r}) - \mathbf{S}_1\mathbf{S}_2\right)\right] - (1 - f_V)\frac{A}{2m^2 r}\mathbf{LS}, \tag{30}$$

where we take the parameter $f_V = 0.7$ for optimal agreement with the experiment. For the dependence of the QCD coupling constant $\tilde{\alpha}_s(\mu^2)$ on the renormalization point μ^2 we use the three-loop result [33]. The typical momentum transfer scale in a quarkonium is of the order of the quark mass, so we set the renormalization scale $\mu = m$ and $\Lambda = 0.168$ GeV. The parameters of the linear confinement potential $A = 0.18$ GeV^2 and $B = -0.16$ GeV have the usual values of quark models.

Using this Hamiltonian, we construct an effective model of the interaction of quarks in a bound state of the Schrödinger type [23,24,34–36]. The numerical solution of the Schrödinger equation, taking into account various corrections in the potential, makes it possible to find the wave function of the bound state, with the help of which the relativistic parameters themselves are then calculated.

The amplitudes of the pair production of vector charmonium and bottomonium in the decay of the Higgs boson are expressed in terms of function $F_{\mathcal{V}\mathcal{V}}$, that is presented in the form of an expansion in $|\mathbf{p}|/m$, $|\mathbf{q}|/m$ up to terms of the second order. As a result of algebraic transformations, it turns out to be convenient to express relativistic corrections in terms of relativistic factors $C_n = (\varepsilon(p) - m)^n/(\varepsilon(p) + m)^n$. As a result of integrating these relativistic factors with the obtained wave functions, we find the values of the relativistic parameters ω_n themselves. In the case of S-states ω_n are determined by the momentum integrals I_n in the form [23,24]:

$$I_n^{\mathcal{P},\mathcal{V}} = \int_0^\infty p^2 R^{\mathcal{P},\mathcal{V}}(p)\frac{(\varepsilon(p)+m)}{2\varepsilon(p)}\left(\frac{\varepsilon(p)-m}{\varepsilon(p)+m}\right)^n dp, \tag{31}$$

$$\tilde{R}(0) = \frac{\sqrt{2}}{\sqrt{\pi}}\int_0^\infty \frac{(\varepsilon(p)+m)}{2\varepsilon(p)}p^2 R(p)dp, \qquad \omega_1^{\mathcal{P},\mathcal{V}} = \frac{I_1^{\mathcal{P},\mathcal{V}}}{I_0^{\mathcal{P},\mathcal{V}}}, \qquad \omega_2^{\mathcal{P},\mathcal{V}} = \frac{I_2^{\mathcal{P},\mathcal{V}}}{I_0^{\mathcal{P},\mathcal{V}}}, \tag{32}$$

where superscripts $\mathcal{P}$, $\mathcal{V}$ denote pseudoscalar and vector states. In the case of quarks of different masses (for B_c mesons), for a mass-symmetric representation of the relativistic parameters, the following equality is used:

$$|\mathbf{p}| = 2m_1\left[\sqrt{\frac{\varepsilon_1 - m_1}{\varepsilon_1 + m_1}} + \left(\frac{\varepsilon_1 - m_1}{\varepsilon_1 + m_1}\right)^{3/2} + \left(\frac{\varepsilon_1 - m_1}{\varepsilon_1 + m_1}\right)^{5/2} + \cdots\right] = \tag{33}$$

$$2m_2\left[\sqrt{\frac{\varepsilon_2 - m_2}{\varepsilon_2 + m_2}} + \left(\frac{\varepsilon_2 - m_2}{\varepsilon_2 + m_2}\right)^{3/2} + \left(\frac{\varepsilon_2 - m_2}{\varepsilon_2 + m_2}\right)^{5/2} + \cdots\right]. \tag{34}$$

TABLE I. Numerical values of the relativistic parameters (25).

$n^{2S+1}L_J$	Meson	$M^{\rm exp}_{Q\bar{Q}}$, GeV	$\tilde{R}(0)$, GeV$^{3/2}$	ω_1	ω_2
1^1S_0	η_c	2.9839	0.92	0.20	0.0087
1^3S_1	J/Ψ	3.0969	0.81	0.20	0.0078
1^1S_0	η_b	9.3987	1.95	0.05	0.0044
1^3S_1	Υ	9.4603	1.88	0.05	0.0044

TABLE II. Numerical results for the decay widths in the nonrelativistic approximation and with the account for relativistic corrections.

Final state $(Q\bar{Q})(Q\bar{Q})$	Nonrelativistic decay width Γ_{nr} in GeV	Relativistic decay width $\Gamma_{\rm rel}$ in GeV
$J/\Psi + J/\Psi$ $1^3S_1 + 1^3S_1$	3.29×10^{-12}	0.69×10^{-12}
$\Upsilon + \Upsilon$ $1^3S_1 + 1^3S_1$	0.63×10^{-12}	0.74×10^{-12}

The Hamiltonian of the system is an important source of relativistic corrections. It allows one to take relativistic effects into account when calculating the wave functions of pseudoscalar and vector mesons (S-states) [25,27,29,32,34,37,38]. The exact form of the bound state wave functions $\Psi_0(\mathbf{q})$ is important to obtain more reliable predictions for the decay widths. In the nonrelativistic approximation the Higgs boson decay width with a production of a pair of quarkonium contains the fourth power of the nonrelativistic wave function at the origin for S-states. The value of the decay width is very sensitive to small changes of $\tilde{R}(0)$. In the nonrelativistic QCD there exists the corresponding problem of determining the magnitude of the color-singlet matrix elements [39].

As a result of the performed transformations, the relativistic parameters are determined by convergent momentum integrals. Their calculation was performed many times for different bound states of quarks in our works [13,15,16]. The numerical values of the parameters ω_1, ω_2 are presented in the Table I. The parameter ω_2 is not included in the decay width, because corrections of the order $O(\mathbf{q}^4)$, $O(\mathbf{p}^4)$ connected with it, are omitted. Using our approach, it is possible to calculate relativistic corrections not only of the second, but also of a higher order.

TABLE IV. The contributions of different mechanisms to the Higgs boson decay widths in GeV.

The contribution accounting for relativistic corrections		
Contribution	$H \to J/\psi\ J/\psi$	$H \to \Upsilon\ \Upsilon$
Figure 1	0.36×10^{-15}	0.10×10^{-12}
Figure 2	0.80×10^{-12}	0.16×10^{-12}
Figure 3	0.70×10^{-13}	0.37×10^{-12}
Figure 4	0.74×10^{-13}	0.68×10^{-13}
Figure 5	0.22×10^{-12}	1.45×10^{-12}
Total contribution	0.69×10^{-12}	0.74×10^{-12}

The results of numerical calculations of the decay widths and parameters A_Q, A_W, B_Q, and B_W are presented in Tables II–IV. Comparing the contributions of different meson pair production mechanisms, it is important to emphasize that their relative magnitude in the total result is determined by such important parameters as α and α_s and the particle mass ratio. So, for example, in the case of the production of a pair of vector mesons, the decay amplitude has two contributions from the quark-gluon (Fig. 1) and quark-photon (Fig. 2) diagrams. On the one hand, the contribution of photon amplitudes is proportional to α, which leads to its decrease in comparison with the contribution from quark-gluon amplitudes. But on the other hand, the quark-photon contribution contains an additional factor $e_Q^2 r_1^2$, which leads to an increase in the decay widths.

IV. CONCLUSION

The study of rare exclusive decay processes of the Higgs boson is an important task, which makes it possible to refine the values of the interaction parameters of particles in the Higgs sector. In this paper, we have attempted to present a complete study of decay processes $H \to J/\Psi J/\Psi$, $H \to \Upsilon\Upsilon$ in the Standard Model by considering the various decay mechanisms shown in Figs. 1–5. To improve the

TABLE III. Numerical values of parameters A and B for W-boson and quark loop mechanisms.

Parameter	$H \to J/\psi\ J/\psi$	$H \to \Upsilon\ \Upsilon$
A_c	$-2.74 \times 10^{-4} + 1.07 \times 10^{-4} i$	$-3.39 \times 10^{-3} + 0.99 \times 10^{-3} i$
A_b	$-5.68 \times 10^{-5} + 7.87 \times 10^{-4} i$	$-1.53 \times 10^{-3} + 0.74 \times 10^{-3} i$
A_t	7.02×10^{-7}	6.54×10^{-6}
A_W	7.94×10^{-5}	7.40×10^{-4}
B_c	$0.31 \times 10^{-4} + 0.62 \times 10^{-10} i$	$0.13 \times 10^{-3} + 0.51 \times 10^{-7} i$
B_b	$-0.42 \times 10^{-7} + 0.42 \times 10^{-10} i$	$0.37 \times 10^{-3} + 0.35 \times 10^{-7} i$
B_t	0.12×10^{-14}	-0.13×10^{-4}
B_W	1.42×10^{-11}	2.76×10^{-4}

calculation accuracy, we take into account relativistic corrections, which were not previously considered in [11,14]. The numerical contribution of different decay mechanisms is analyzed and it is shown that in the case of double production of charmonium, the main decay mechanism is the quark-photon one in Fig. 2, ZZ-mechanism in Fig. 5. However, it is also necessary to take into account other mechanisms to achieve high calculation accuracy (see also [22]). For bottomonium pair production all mechanisms give close contributions to the width, but the ZZ-mechanism is dominant. Their sum ultimately determines the full numerical result. The parameters A_W, A_Q, B_W, and B_Q, which determine the numerical values of the contributions of the W-boson loop mechanism and the quark loop mechanism, are obtained in analytical and numerical form. They are presented separately in Table III.

In our approach, we distinguish two types of relativistic corrections. The corrections of the first type are determined by the relative momenta p and q in the production amplitude of two quarks and two antiquarks. The corrections of the second type are determined by the transformation law of the meson wave functions, which results in expressions (5)–(6). The $\Psi_0(\mathbf{p})$ wave functions entering into (5)–(6) in the rest frame of the bound state are found from the solution of the Schrödinger equation with a potential that includes relativistic corrections. Having an exact expression for the decay amplitude (see the example in Appendix C), we carry out a series of transformations with it, extracting second-order corrections in p and q. The model used is described in more detail in [13]. In our approach, all arising relativistic parameters ω_1, ω_2, $\tilde{R}(0)$ are determined within the framework of the relativistic quark model (see Table I). Accounting for relativistic corrections in this work shows that such contributions lead to a significant change in nonrelativistic results. Here it must be emphasized that we call nonrelativistic results such results that are obtained at $p = 0$, $q = 0$ and neglecting relativistic corrections in the quark interaction potential. The main parameter that greatly reduces the nonrelativistic results is $\tilde{R}(0)$, which enters in the decay width to the fourth power. Therefore, the difference between the relativistic and nonrelativistic results in Table II turns out to be more significant in the case of pair production of charmonium.

The paper considers various mechanisms for the production of a pair of vector mesons in the decay of the Higgs boson, which are presented in Figs. 1–5. The decay branchings are equal: $\mathrm{Br}(H \to J/\Psi J/\Psi) = 2.1 \times 10^{-10}$, $\mathrm{Br}(H \to \Upsilon\Upsilon) = 2.3 \times 10^{-10}$. There are other amplitudes for the production of a pair of J/Ψ, Υ mesons, which are calculated but not included in detail in the work. So, for example, there is a pair production mechanism (HH mechanism), when the original Higgs boson turns into a HH pair, which then gives a pair of vector mesons in the final state. In a sense, it is similar to the ZZ mechanism, but the amplitude structure is different, which results to a contribution to the decay width that is several orders of magnitude smaller than those given in Table I. Despite the obvious difference in the amplitudes in Figs. 1 and 2 in terms of the mass factor M^2/M_h^2, we include the amplitudes of Fig. 1 in the consideration, in contrast to work [14]. We do not consider amplitudes like those shown in Fig. 3, but with two gluons. In this case, the direct amplitude [Fig. 3 (left)] vanishes due to the color factor, and the cross amplitude [Fig. 3 (right)] is suppressed by the mass factor M^2/M_h^2. A distinctive feature of our calculations is that when studying the contributions of the amplitudes in Figs. 3–4, we take into account two structure functions A_i and B_i ($i = W$, Q) (15) in the tensor function of the triangular loop. They are calculated analytically and numerically, and the corresponding results are presented in Table IV and Appendixes A and B. Although the function B_i initially contains higher powers of the factor r_4 (see Appendixes A and B), which should lead to a decrease in the numerical values for $r_4 \ll 1$, nevertheless, the structure of the coefficient functions in (25) is such that the function B_i cannot be neglected.

In Table IV, we present separately the numerical values of the contributions from different decay mechanisms with an accuracy of two significant figures after the decimal point. First of all, the problem was to obtain the main contribution to the decay width. This was the contribution from the quark-photon mechanism in Fig. 2 and the ZZ mechanism in Fig. 5, which are one order of magnitude greater than the other contributions in the case of charmonium production. Its value is due to the structure of the decay amplitudes, in which small denominators $1/M^2$ appear from the photon propagators in contrast to other amplitudes in which there is a factor $1/M_H^2$. In addition, the numerator in these amplitudes contains amplifying factors in powers of a large parameter r_1. In each considered decay mechanism, there are radiative corrections $O(\alpha_s)$ that were not taken into account. They represent a major source of theoretical uncertainty, which we estimate to be about 30% in α_s. Other available errors connected with the parameters of the Standard Model and higher-order relativistic corrections do not exceed 10%. On the whole, our complete numerical estimates of the decay widths agree in order of magnitude with the results [14].

The obtained values for the decay width of the Higgs boson into a pair of charmoniums or bottomonions allow us to give a numerical estimate of the possible number of such events in future Higgs boson factories. The parameters of future colliders (ILC, FFC, etc.) are still under discussion [40,41]. In the case of pp-colliders at high luminosities, the production of 4×10^{10} Higgs bosons per year is possible. Then, taking into account the value of the total Higgs boson decay width, we can expect about 10 Higgs boson decays into charmonium pair per year.

ACKNOWLEDGMENTS

The work is supported by the Foundation for the Advancement of Theoretical Physics and Mathematics "BASIS" (Grant No. 22-1-1-23-1). The authors are grateful to A. V. Berezhnoy, I. N. Belov, D. Ebert, V. O. Galkin, A. K. Likhoded for useful discussions.

APPENDIX A: THE CALCULATION OF W-BOSON LOOPS BY THE DISPERSION METHOD

In Appendixes A and B we consider the calculation of tensors that determine the contributions to the Higgs boson decay width from the two mechanisms shown in Figs. 3 and 4 (see also [42–52]).

The Higgs boson decay amplitude into two charmonium states contains the contribution which is determined by W-boson loop presented in Fig. 4. Generally speaking, along with W-boson loops, it is also necessary to consider other many-numbered loop contributions determined by Goldstone bosons and ghosts. But there is a unitary gauge convenient for calculation, in which there is only the contribution of the diagrams presented in Fig. 4.

The tensor corresponding to triangle loop can be written as follows:

$$T^{\mu\nu}_{1,W}=8\pi\alpha M_Z M_W(\sqrt{2}G_F)^{1/2}\cos\theta_W\int\frac{d^4k}{(2\pi)^4}\frac{V_{\mu\sigma\rho}(r-k,P,Q-k)V_{\nu\omega\lambda}(Q-k,Q,-k)}{(k^2-M_W^2)((r-k)^2-M_W^2)((Q-k)^2-M_W^2)}$$
$$\times\left[g^{\rho\omega}-\frac{(Q-k)^\rho(Q-k)^\omega}{M_W^2}\right]\left[g^{\lambda\alpha}-\frac{(r-k)^\lambda(r-k)^\alpha}{M_W^2}\right]\left[g^{\sigma\alpha}-\frac{k^\sigma k^\alpha}{M_W^2}\right]+(\mu\leftrightarrow\nu,P\leftrightarrow Q). \tag{A1}$$

The tensor $T^{\mu\nu}_{2,W}$ of second Feynman amplitude in Fig. 4 has the similar form. Next, we consider the sum of these two amplitudes.

To calculate the tensor $T^{\mu\nu}_W$ of bosonic loop, we use the dispersion method, keeping in mind that the tensor that defines this loop has the general structure (15). Then the structure functions $A_W(t)$, $B_W(t)$ can be obtained by performing the following convolutions over the Lorentz indices:

$$A_W(t)=T^{\mu\nu}\frac{1}{2}\left[\frac{g^{\mu\nu}}{v_1v_2}-\frac{v_1^\nu v_2^\mu}{(v_1v_2)^2-1}\right],\qquad B_W(t)=T^{\mu\nu}\frac{1}{2}\left[\frac{3v_1^\nu v_2^\mu}{((v_1v_2)^2-1)^2}-\frac{g^{\mu\nu}}{v_1v_2((v_1v_2)^2-1)}\right]. \tag{A2}$$

For two structure functions $A_W(t)$, $B_W(t)$ we use the dispersion relation with one subtraction,

$$A_W(t)=A_W(0)+\frac{t}{\pi}\int_1^\infty\frac{\mathrm{Im}A(t')dt'}{t'(t'-t+i0)},\qquad B_W(t)=B_W(0)+\frac{t}{\pi}\int_1^\infty\frac{\mathrm{Im}B(t')dt'}{t'(t'-t+i0)}. \tag{A3}$$

Imaginary parts $\mathrm{Im}A(t)$, $\mathrm{Im}B(t)$ can be calculated using the Mandelstam-Cutkosky rule [53,54]. For example, the imaginary part of the function $A(t)$ is equal,

$$\mathrm{Im}A_W=\frac{r_3^2}{512\pi\sqrt{t(t-1)}(2t-r_3^2)(t-r_3^2)^{3/2}}\left\{4r_3^2(1-t)(t-r_3^2)^{1/2}[r_3^2(4+r_3^2-2t)(2t+1)-4(2t+3)]\right.$$
$$+\sqrt{t-1}[8r_3^6+48(1-2t)t+r_3^8(1+2t)-4r_3^4(3+t)(3+2t)+16r_3^2(-3+t(9+2t))]$$
$$\left.\times\ln\frac{r_3^2-2t+2\sqrt{(t-1)(t-r_3^2)}}{r_3^2-2t-2\sqrt{(t-1)(t-r_3^2)}}\right\},\qquad r_3=\frac{M}{M_W},\qquad M=M_{Q\bar{Q}}. \tag{A4}$$

This expression accurately takes into account the dependence on the meson mass M. Accounting for $r_3\ll1$, we can perform an expansion in r_3,

$$\mathrm{Im}A_W(t)=\frac{1}{16\pi}\left\{\frac{3r_3^2}{4}\frac{(2t-1)\ln\frac{\sqrt{t}+\sqrt{t-1}}{\sqrt{t}-\sqrt{t-1}}}{t^2}+\frac{r_3^4}{t^3\sqrt{t-1}}\left[\sqrt{t}(2t^2+t-3)-\sqrt{t-1}(3-3t+2t^2)\ln\frac{\sqrt{t}+\sqrt{t-1}}{\sqrt{t}-\sqrt{t-1}}\right]\right\}. \tag{A5}$$

Calculating the dispersion integral with subtraction, we get,

$$A_W(t) = \frac{1}{16\pi^2} r_3^2 \tilde{A}_W(t) = \frac{1}{16\pi^2} r_3^2 \left\{ \frac{3}{t^2}[t + (2t-1)f(t)^2] - 5 \right\} + \frac{1}{16\pi^2} \frac{2r_3^4}{15t^4} \left\{ 90t - 15t^2 + 7t^3 + 15f(t) \left[\frac{(2t^2+t-3)}{\sqrt{t-1}t^{7/2}} + (-3+3t-2t^2)f(t) \right] \right\}, \tag{A6}$$

$$f(t) = \begin{cases} \arcsin\sqrt{t}, & t \le 1, \\ \frac{i}{2}\left[\ln\frac{1+\sqrt{1-t^{-1}}}{1-\sqrt{1-t^{-1}}} - i\pi \right], & t > 1, \end{cases} \tag{A7}$$

$$B_W(t) = \frac{1}{16\pi^2} \frac{r_3^6}{210t^9(1-t)} \left\{ t^5(t-1)[-t(1470 + t(2051 + 1943t)) + 210\ln(1-t) \times (-6_t(-4 + t(-3+2t))) + 4\ln 2(315 + t(735 + 44t(7+16t)))] + 105i\sqrt{t^9(1-t)}(3 + 5t - 2t^2 + 4t^3) \times \left[\ln 2 \ln\frac{1-2t-2i\sqrt{t(1-t)}}{1-2t+2i\sqrt{t(1-t)}} + 2\mathrm{Li}_2(t - i\sqrt{t(1-t)}) - 2\mathrm{Li}_2(t + i\sqrt{t(1-t)}) - \mathrm{Li}_2(2t - 2i\sqrt{t(1-t)}) + \mathrm{Li}_2(2t + 2i\sqrt{t(1-t)}) \right] \right\}. \tag{A8}$$

The subtraction constant $\tilde{A}_W(0) = 7$. Then, in the leading order in r_3, the function $A_W(t)$ is equal to

$$A_W(t) = \frac{1}{16\pi^2} r_3^2 \left[2 + \frac{3}{t} + \frac{3}{t^2}(2t-1)f(t)^2 \right]. \tag{A9}$$

The limit $M_W \to 0$ within the Goldstone-boson approximation gives $\tilde{A}_W|_{M_W \to 0} \to 2$. The numerical value of $B_W(t)$ is significantly less than (A6) due to the factor r_3^6.

APPENDIX B: THE CALCULATION OF QUARK LOOPS BY THE DISPERSION METHOD

The calculation of the quark loops contribution to structure functions $A_Q(t)$, $B_Q(t)$ can be carried out also by dispersion method. Final expression for imaginary parts of these functions are the following:

$$\mathrm{Im}A_Q = -\frac{r_4^2}{512\pi\sqrt{t}(2t-r_4^2)(t-r_4^2)^2} \left\{ 4r_4^2(r_4^2 - t)\sqrt{t-1} + \sqrt{t-r_4^2}[r_4^4 + r_4^2(4-6t) + 4t(t-1)] \ln\frac{r_4^2 - 2t + 2\sqrt{(t-1)(t-r_4^2)}}{r_4^2 - 2t - 2\sqrt{(t-1)(t-r_4^2)}} \right\}, \qquad r_4 = \frac{M}{m_Q}, \tag{B1}$$

$$\mathrm{Im}B_Q = \frac{r_4^6}{256\pi t^{3/2}(2t-r_4^2)(t-r_4^2)^{5/2}} \left\{ -4(r_4^2 - 4t)\sqrt{(t-1)(t-r_4^2)} + [r_4^4 + 4t(1+2t) - 2r_4^2(2+3t)] \ln\frac{r_4^2 - 2t + 2\sqrt{(t-1)(t-r_4^2)}}{r_4^2 - 2t - 2\sqrt{(t-1)(t-r_4^2)}} \right\}, \qquad r_4 = \frac{M}{m_Q}, \tag{B2}$$

where m_Q is the mass of heavy quarks in the loop.

In the case of quark loops, we use the dispersion relation without subtractions. The functions $A_Q(t)$ and $B_Q(t)$ have the following explicit form after expansion in r_4^2:

$$A_Q(t) = -\frac{1}{16\pi^2} \frac{r_4^2}{32t^3} \{4t^2 + 4t(t-1)f^2(t) + r_4^2[-2t(t-4) - 4\sqrt{t(1-t)}f(t) + 2(t-2)f^2(t)]\}, \tag{B3}$$

$$B_Q(t) = -\frac{1}{16\pi^2}\frac{r_4^6}{2520t^5}\Big\{2t[-14t(225+t(45+14t)) - r_4^2(6930+t(1365+t(413+216t)))] + 1260\Big[9r_4^2\sqrt{(1-t)t}+4\sqrt{(1-t)t^3}\Big]f(t) + 630(2t(1+2t)+r_4^2(4+9t))f^2(t)\Big\}. \tag{B4}$$

In the leading order in r_4^2 the expression (B2) coincides with the known expression obtained in [42–51]. Since $B(t)$ contains the factor r_4 to a higher degree, its contribution is sometimes neglected.

APPENDIX C: THE AMPLITUDE OF PAIR VECTOR MESONS PRODUCTION VIA THE ZZ MECHANISM

The amplitude of direct production of vector mesons [Fig. 5 (left)] has the form,

$$\mathcal{M}_{\rm dir} = \frac{48\pi\alpha(\sqrt{2}G_F)^{1/2}M_Z^2}{\sin^2 2\theta_W}\int\frac{d\mathbf{p}}{(2\pi)^3}\frac{\Psi_0(\mathbf{p})}{\frac{\epsilon(p)}{m}\frac{(\epsilon(p)+m)}{2m}}\int\frac{d\mathbf{q}}{(2\pi)^3}\frac{\Psi_0(\mathbf{q})}{\frac{\epsilon(q)}{m}\frac{(\epsilon(q)+m)}{2m}}D_{\mu\alpha}(P)D_{\nu\alpha}(Q)$$
$$\times{\rm Tr}\Big\{\Big[\frac{\hat v_1-1}{2}-\frac{\hat v_1 p^2}{2m(\epsilon(p)+m)}-\frac{\hat p}{2m}\Big]\hat\varepsilon_1(\hat v_1+1)\Big[\frac{\hat v_1-1}{2}-\frac{\hat v_1 p^2}{2m(\epsilon(p)+m)}+\frac{\hat p}{2m}\Big]\gamma_\mu\Big[\frac{1-\gamma_5}{2}-a_z\Big]\Big\}$$
$$\times{\rm Tr}\Big\{\Big[\frac{\hat v_2-1}{2}-\frac{\hat v_2 q^2}{2m(\epsilon(q)+m)}-\frac{\hat q}{2m}\Big]\hat\varepsilon_2(\hat v_2+1)\Big[\frac{\hat v_2-1}{2}-\frac{\hat v_2 q^2}{2m(\epsilon(q)+m)}+\frac{\hat q}{2m}\Big]\gamma_\nu\Big[\frac{1-\gamma_5}{2}-a_z\Big]\Big\}, \tag{C1}$$

where $\varepsilon_{1,2}$ are the polarization four-vectors describing vector meson states. $D_{\mu\alpha}(k)$ is the Z-boson propagator.

The amplitude of crossed production of vector mesons (Fig. 5 (right)) has the form:

$$\mathcal{M}_{cr} = \frac{16\pi\alpha(\sqrt{2}G_F)^{1/2}M_Z^2}{\sin^2 2\theta_W}\int\frac{d\mathbf{p}}{(2\pi)^3}\frac{\Psi_0(\mathbf{p})}{\frac{\epsilon(p)}{m}\frac{(\epsilon(p)+m)}{2m}}\int\frac{d\mathbf{q}}{(2\pi)^3}\frac{\Psi_0(\mathbf{q})}{\frac{\epsilon(q)}{m}\frac{(\epsilon(q)+m)}{2m}}D_{\mu\alpha}(P)D_{\nu\alpha}(Q)$$
$$\times{\rm Tr}\Big\{\Big[\frac{\hat v_1-1}{2}-\frac{\hat v_1 p^2}{2m(\epsilon(p)+m)}-\frac{\hat p}{2m}\Big]\hat\varepsilon_1(\hat v_1+1)\Big[\frac{\hat v_1-1}{2}-\frac{\hat v_1 p^2}{2m(\epsilon(p)+m)}+\frac{\hat p}{2m}\Big]\gamma_\mu\Big[\frac{1-\gamma_5}{2}-a_z\Big]$$
$$\times\Big[\frac{\hat v_2-1}{2}-\frac{\hat v_2 q^2}{2m(\epsilon(q)+m)}-\frac{\hat q}{2m}\Big]\hat\varepsilon_2(\hat v_2+1)\Big[\frac{\hat v_2-1}{2}-\frac{\hat v_2 q^2}{2m(\epsilon(q)+m)}+\frac{\hat q}{2m}\Big]\gamma_\nu\Big[\frac{1-\gamma_5}{2}-a_z\Big]\Big\}. \tag{C2}$$

After all the transformations, the total amplitude of the production of a pair of vector mesons in the ZZ mechanism takes the form (18).

[1] G. Aad *et al.* (the ATLAS Collaboration), Phys. Lett. B **716**, 1 (2012).
[2] S. Chartchyan *et al.* (the CMS Collaboration), Phys. Lett. B **716**, 30 (2012).
[3] CMS Collaboration, Nature (London) **607**, 60 (2022).
[4] P. A. Zyla *et al.* (Particle Data Group), Prog. Theor. Exp. Phys. **2020**, 083C01 (2020).
[5] K. Abe (Belle Collaboration) *et al.*, Phys. Rev. D **70**, 071102 (2004).
[6] B. Aubert (*BABAR* Collaboration) *et al.*,Phys. Rev. D **72**, 031101 (2005).
[7] A. M. Sirunyan *et al.* (CMS Collaboration), Phys. Lett. B **797**, 134811 (2019).
[8] CMS Collaboration, arXiv:2206.03525v1.
[9] M. Bander and A. Soni, Phys. Lett. **82B**, 411 (1979).
[10] W. Y. Keung, Phys. Rev. D **27**, 2762 (1983).
[11] V. Kartvelishvili, A. V. Luchinsky, and A. A. Novoselov, Phys. Rev. D **79**, 114015 (2009).
[12] I. N. Belov, A. V. Berezhnoy, A. E. Dorokhov *et al.*, Nucl. Phys. **A1015**, 122285 (2021).
[13] R. N. Faustov, F. A. Martynenko, and A. P. Martynenko, Eur. Phys. J. A **58**, 1 (2022).
[14] D.-N. Gao and X. Gong, Phys. Lett. B **832**, 137 (2022).
[15] A. E. Dorokhov, R. N. Faustov, A. P. Martynenko, and F. A. Martynenko, Phys. Rev. D **102**, 016027 (2020).
[16] E. N. Elekina and A. P. Martynenko, Phys. Rev. D **81**, 054006 (2010).
[17] A. P. Martynenko and A. M. Trunin, Phys. Rev. D **86**, 094003 (2012).
[18] G. T. Bodwin and A. Petrelli, Phys. Rev. D **66**, 094011 (2002).

[19] S. J. Brodsky and J. R. Primack, Ann. Phys. (N.Y.) **52**, 315 (1969).
[20] R. N. Faustov, Ann. Phys. (N.Y.) **78**, 176 (1973).
[21] J. Kuipers, T. Ueda, J. A. M. Vermaseren, and J. Vollinga, Comput. Phys. Commun. **184**, 1453 (2013).
[22] G. T. Bodwin, H. S. Chung, J.-H. Ee, J. Lee, and F. Petriello, Phys. Rev. D **90**, 113010 (2014).
[23] A. V. Berezhnoy, A. P. Martynenko, F. A. Martynenko, and O. S. Sukhorukova, Nucl. Phys. **A986**, 34 (2019).
[24] A. A. Karyasov, A. P. Martynenko, and F. A. Martynenko, Nucl. Phys. **B911**, 36 (2016).
[25] S. N. Gupta, S. F. Radford, and W. W. Repko, Phys. Rev. D **26**, 3305 (1982).
[26] W. Lucha, F. F. Schöberl, and D. Gromes, Phys. Rep. **200**, 127 (1991).
[27] N. Brambilla, A. Pineda, J. Soto, and A. Vairo, Rev. Mod. Phys. **77**, 1423 (2005).
[28] K. Melnikov and A. Yelkhovsky, Phys. Rev. D **59**, 114009 (1999).
[29] S. Godfrey and N. Isgur, Phys. Rev. D **32**, 189 (1985).
[30] S. F. Radford and W. W. Repko, Phys. Rev. D **75**, 074031 (2007).
[31] S. N. Gupta, Phys. Rev. D **35**, 1736 (1987).
[32] S. N. Gupta, J. M. Johnson, W. W. Repko, and C. J. Suchyta, Phys. Rev. D **49**, 1551 (1994).
[33] K. G. Chetyrkin, B. A. Kniehl, and M. Steinhauser, Phys. Rev. Lett. **79**, 2184 (1997).
[34] W. Lucha and F. F. Schöberl, Phys. Rev. A **51**, 4419 (1995).
[35] W. Lucha and F. F. Schöberl, Int. J. Mod. Phys. C **10**, 607 (1999).
[36] P. Falkensteiner, H. Grosse, F. F. Schöberl, and P. Hertel, Comput. Phys. Commun. **34**, 287 (1985).
[37] D. Ebert, R. N. Faustov, and V. O. Galkin, Eur. Phys. J. C **71**, 1825 (2011).
[38] D. Ebert, R. N. Faustov, V. O. Galkin, and A. P. Martynenko, Phys. At. Nucl. **68**, 784 (2005).
[39] G. T. Bodwin, E. Braaten, and G. P. Lepage, Phys. Rev. D **51**, 1125 (1995).
[40] J. de Blas, R. Franceschini, F. Riva, P. Roloff, U. Schnoor *et al.*, CERN Yellow Rep. Monogr. **3**, 1 (2018).
[41] R. Contino, D. Curtin, A. Katz, M. L. Mangano, G. Panico *et al.*, CERN Yellow Rep. **3**, 255 (2017).
[42] J. Horejsi and M. Stöhr, Phys. Lett. B **379**, 159 (1996).
[43] L. Bergström and G. Hulth, Nucl. Phys. **B259**, 137 (1985).
[44] A. P. Martynenko and R. N. Faustov, Moscow Univ. Phys. Bull. **53**, 6 (1998).
[45] I. Boradjiev, E. Christova, and H. Eberl, Phys. Rev. D **97**, 073008 (2018).
[46] E. Christova and I. Todorov, Bulg. J. Phys. **42**, 296 (2015).
[47] M. A. Shifman, A. I. Vainshtein, M. B. Voloshin, and V. I. Zakharov, Yad. Fiz. **30**, 1368 (1979) [Sov. J. Nucl. Phys. **30**, 711 (1979)].
[48] W. J. Marciano, C. Zhang, and S. Willenbrock, Phys. Rev. D **85**, 013002 (2012).
[49] K. Melnikov and A. Vainshtein, Phys. Rev. D **93**, 053015 (2016).
[50] J. G. Körner, K. Melnikov, and O. I. Yakovlev, Phys. Rev. D **53**, 3737 (1996).
[51] K. Melnikov, M. Spira, and O. I. Yakovlev, Z. Phys. C **64**, 401 (1994).
[52] R. Gastmans, S. L. Wu, and T. T. Wu, Int. J. Mod. Phys. A **30**, 1550200 (2015).
[53] R. E. Cutkosky, J. Math. Phys. (N.Y.) **1**, 429 (1960).
[54] V. B. Berestetskii, E. M. Lifshits, and L. P. Pitaevskii, *Quantum Electrodynamics* (Nauka, Moscow, 1980).